Tech Science Press

# Compression Behaviors of Parallel Bamboo Strand Lumber Under Static Loading

**Haitao Li[1,2,*], Zhenyu Qiu[2], Gang Wu[1,*], Dongdong Wei[3], Rodolfo Lorenzo[4], Conggan Yuan[3], Huizhong Zhang[1,2] and Rong Liu[1,2]**

[1]Southeast University, Key laboratory of concrete and pre-stressed concrete structure of Ministry of Education, Nanjing, 210096, China; College of Civil Engineering, Nanjing Forestry University, Nanjing, 210037, China.

[2]Department of Building Engineering, Nanjing Forestry University, Nanjing, 210037, China.

[3]Jiangxi Feiyu Bamboo Stock Co. LTD, Fengxin, 330700, China.

[4]University College London, London WC1E 6BT, UK.

[*]Corresponding Authors: Haitao Li. Email: lhaitao1982@126.com; Gang Wu. Email: g.wu@seu.edu.cn.

**Abstract:** In order to investigate the influence of length and compression directions upon behaviour of parallel bamboo strand lumber (PBSL) specimens, 240 axial compression tests have been performed. With three similar one different typical failure modes, the mechanical performance for PBSL specimens under compression parallel to grain and perpendicular to grain are different as a whole. From the point of the characteristic values, the compression strength parallel to grain is 2.1 times of the compression strength perpendicular to grain. The elastic modulus for compression parallel to grain is 3.64 times of the compression strength perpendicular to grain. While the compression ratios along two compression directions are equal to each other. The bigger Poisson ratios for one typical side surface is 3.93 times of that for another typical side surface for PBSL specimens under compression perpendicular to grain, and the bigger value is equal to that for PBSL specimens under compression parallel to grain. Length can influence the mechanical properties of the PBSL specimens. The size 50 mm × 50 mm × 100 mm should be good choice for the standard or code to measure the compression strength. PBSL materials have better ductility under compression parallel to grain than that under compression perpendicular to grain. Stress-strain relationship models were proposed for PBSL specimens under compression parallel to grain and perpendicular to grain, respectively. These proposed models gave a good agreement with the test results.

**Keywords:** Parallel bamboo strand lumber; compression; parallel to grain; perpendicular to grain; stress-strain relationship model

## 1 Introduction

With the deterioration of the environment, more and more scientists in civil engineering field are paying attention to the green building materials such as timer [1-2], bamboo [3-13], straw and so on. This paper will mainly present the study on the compression performance of parallel bamboo strand lumber (PBSL) [14-17] which could be made by gluing the bamboo filament bundles together [17].

Considering some influencing factors, the mechanical properties for PBSL have been studied. Huang [18] investigated the basic material performance and the aging resistant performance of PBSL. Liang Cheng [19] has studied the manufacturing technology for PBSL considering the bamboo bundle preparation, glue immersion, forming and hot pressing process. Naresworo Nugroho et al. [20-21] have performed a study to determine the suitability of zephyr strand from moso bamboo *(Pyllostachys*

DOI: 10.32604/jrm.2019.07592 

*pubescens* Mazel) for structural composite board manufacture. Cui et al. [22] found that the presence of prestress in bamboo slivers reinforced parallel strand lumber (PSL) could enhance its flexural stiffness and toughness but not the flexural strength. Pannipa Malanit et al. [23] found that the resin type has a significant effect on oriented strand lumber (OSL) board properties. Zhou et al. [24] studied the mode-I fracture properties of PBSL. Shangguan et al. [25] proposed strength models of PBSL for compressive properties. Zhong et al. [26-27] investigated the effects of temperature on the compressive strength parallel to the grain of PBSL as well as its design value. Ahmad et al. [28] have analyzed the physical and mechanical properties of parallel strand lumber (PSL) made from Calcutta bamboo. Xu et al. [29] have studied compressive and tensile properties of PBSL at elevated temperatures. Yu et al. [30-31] have carried out the experiments about the preparation, physical, mechanical, and interfacial morphological properties of PBSL. Considering some influencing factors, the mechanical performance for PBSL columns [16-17] and beams [32-34] were also investigated by the researchers.

As discussed above, even though the mechanical properties for PBSL have been studied considering many influencing factors, a good constitutive model for PBSL is still lack. None specific test standard for PBSL in structural use existed in the world. A good size for measuring the compression strength is very important to write the code. To achieve these aims, the study investigates in detail how length and compression directions influence upon behaviour of parallel bamboo strand lumber (PBSL) specimens.

## 2 Materials and Test Methods

The source Moso bamboo (Phyllostachys pubescens, from Feng-xin county in the Jiang-xi province) was harvested at the age of 3-4 years. Bamboo strips from the upper growth heights, of a 2000 mm tall culm were selected. The culms cut from assigned growth portions were then split into 20 mm wide strips, and the outer skin (epidermal) and inner cavity layer (pith peripheral) were removed using a planer. All culm strips were split into bamboo filament bundles by passing through a roller press crusher. Then these bamboo filament bundles were dried and charred under the temperature of 165 degree centigrade and air pressure of 0.3 MPa. Finally the bundles (Fig. 1) were made into parallel bamboo strand lumber lumbers by Fei-yu Co. Ltd.

(a) Bamboo strand bundles (b) Molds for PBSL

(c) Hot pressing (d) PBSL (e) Cross-section for PBSL

**Figure 1:** Main manufacturing process for parallel bamboo strand lumber (PBSL)

Phenol glue was used to manufacture the parallel bamboo strand lumber specimens. All bundles were put into many molds (Fig. 1(b)), and these were then pressed together to form the blocks. A transverse compression of 10.3 MPa was applied for the blocks under the hot pressing temperature with the value of 160℃. The final moisture content was 8.22% and the density was 1250 kg/m$^3$ for the laminate sourced from the upper portion.

Considering the length and compression directions, six groups of specimens were constructed and detailed information could be seen in Tab. 1. As for the naming rule for the groups, "CS + length" is for the group under compression parallel to grain and "CH + length" is for the group under compression perpendicular to grain. In addition, the "length" is the compression direction. Each group consisted of 40 identical specimens.

**Table 1:** Details of the test specimens

| Specimen group | Width *b* (mm) | Height *H* (mm) | Length *L* (mm) | Number of specimen |
|---|---|---|---|---|
| CS100 | 50 | 50 | 100 | 40 |
| CS150 | 50 | 50 | 150 | 40 |
| CS200 | 50 | 50 | 200 | 40 |
| CH100 | 50 | 50 | 100 | 40 |
| CH150 | 50 | 50 | 150 | 40 |
| CH200 | 50 | 50 | 200 | 40 |

The test arrangement is illustrated in Fig. 2. The displacement along axial direction of the specimen was measured by two Laser Displacement Sensors (LDS). Two strain gauges were pasted on each middle side surface of the specimens, as shown in Fig. 2. The test was performed using a microcomputer-controlled electro-hydraulic servo universal testing machine with a capacity of 2000 kN and an TDS Data Acquisition System.

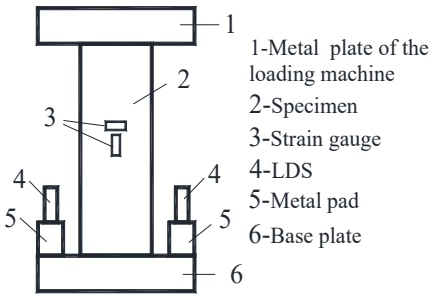


**Figure 2:** Test scheme

The total loading duration is controlled between 8-10 minutes. The load was applied initially through load control in the elastic stage, and then was changed to displacement control before the proportional limit. The load was ramped up linearly to 100 kN at a rate of 1.0 kN/sec, after which the testing process was changed to displacement control. The test continued at a displacement rate of 0.02 mm/sec until the specimen had sustained significant damage, at which time testing was halted.

## 3 Test Results and Analysis

### *3.1 Failure Phenomena Analysis*

Similar to other kinds of engineered bamboo materials [3-8], all PBSL specimens experienced elastic stage firstly and then elastic-plastic stage. None obvious failure phenomena on the surfaces could be seen both for elastic stage and elastic-plastic stage. But a clear voice could be heard when the loading value increased about 70% of the ultimate load. Some minor cracks might be appeared in the inner part of the specimens. With the increase of loading, cracks appeared on the surface of the specimens. However, the final failure phenomena varied greatly. Detailed analysis about the final phenomena will be discussed in the following. Four side surfaces of the specimens were named as A, B, C, D (Fig. 3) so that the description of the failure phenomena for each specimens could be done easily [35].

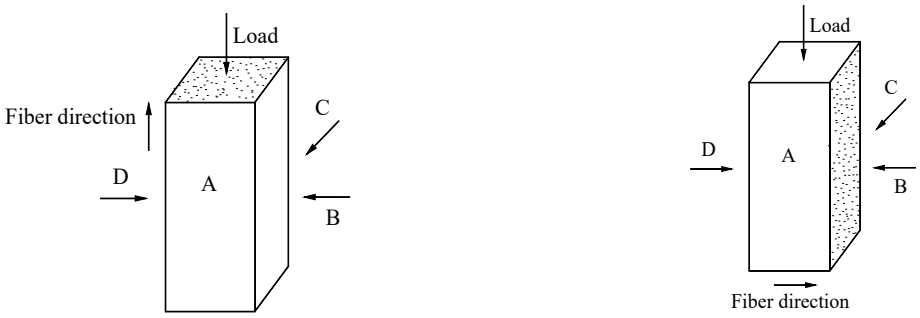


(a) Specimens for compression parallel to grain (b) Specimens for compression perpendicular to grain

**Figure 3:** Number for four side surfaces

#### *3.1.1 Compression Parallel to Grain*

According to the failure process for all specimens, two main failure phenomena series could be classified which are axial compression strength failure and buckling failure. Only strength failure happed for group CS100 and CS150, but both failures occurred for group CS200. Four typical failure modes could be divided into for axial compression strength failures, which were shown from Fig. 4. And detailed failure modes information for each group could be seen from Tab. 2.

As for mode I shown in Fig. 4(a), the shape for the main cracks looks like “Y”. Cracks appeared firstly from the two top corners. With the increase of loading, more and more cracks appeared along the two corner angular surfaces. Two cracks surfaces met at the central in the middle axis line along the length of the specimens. Then the cracks surface developed from the cross point line to the bottom along the vertical axis line. There are 7 specimens damaged as this mode for group CS100, 11 for CS150 and 4 for group CS200. The total number for mode I is 22 which is 18.33% of 120 specimens.

(a) Mode Ⅰ (b) Mode Ⅱ (c) Mode Ⅲ (d) Mode Ⅳ

**Figure 4:** Typical failure modes for axial compression strength failure

Typical failure mode II could be seen from Fig. 4(b). Cracks appeared firstly just from one top corners or one side of the specimens and then extended along one corner angular surfaces with the increase of loading. Only one main cracks line could be seen from the surface of the specimen in the final failure photo and the line crossed through D surface. Group CS100 has 16 specimens damaged with mode II. Group CS150 and CS200 have 19 and 6 specimens respectively. With the total number of 41, specimens of mode II account for 34.17% of 120 specimens.

Fig. 4(c) shows typical failure for mode III. Similar to mode II, cracks appeared firstly just from one top corners and extended along one corner angular surfaces with the increase of loading. However, this cracks line stoped along the original direction when it achieved close middle point and then developed along the central line or parallel to the central line from the middle to the bottom. The numbers for mode III are 15, 6, 5 for group CS100, CS150 and CS200 respectively. And the total number is 26 which is 21.67% of 120 specimens damaged with this failure mode.

Mode IV could be called split failure. All cracks developed along the vertical length direction of the specimen with the increase of loading, as shown in Fig. 4(d). With the number of 2 for group CS100, the number of 4 for CS150 and the number of 13 for group CS200, the total number for mode IV is 19. That is to say 15.83% of 120 specimens damaged with this failure mode.

**Table 2:** Failure modes numbers for each group under compression parallel to grain

| Specimen group | Mode I | Mode II | Mode III | Mode IV | Total |
|---|---|---|---|---|---|
| CS100 | 7 | 16 | 15 | 2 | 40 |
| CS150 | 11 | 19 | 6 | 4 | 40 |
| CS200 | 4 | 6 | 5 | 13 | 28 |
| Total | 22 | 41 | 26 | 19 | 108 |

As can be seen from Tab. 2, 108 specimens damaged with axial compression strength failure which take the percentage of 90% in 120 specimens. And the left 12 specimens failed as the buckling failure. As for this failure mode, lateral deformation occurred for all 12 specimens firstly and then some cracks appeared in the specimens. All these specimens belong to group CS200. That is to say 50 by 50 by 200 mm is not good size for the specimen to measure the compression strength parallel to grain in a standard or code.

### *3.1.2 Compression Perpendicular to Grain*

Similar to the failure for compression parallel to grain, both axial compression strength failure and buckling failure occurred for the specimens under compression perpendicular to grain. However, only several specimens from group CH200 failed as the buckling failure and all other specimens have strength failure modes. Fig. 5 shows four typical failure modes for axial compression strength failures and detailed failure modes information could be seen from Tab. 3.

As shown in Fig. 5, the first three failure modes are similar to those for the specimens under compression parallel to grain. However, as for mode I, cracks appeared firstly from the middle parts of the specimens but not from the two top corners. There are 6 specimens failed as mode I for group CH100, 13 for group CH150 and 4 for group CH200. The total number for mode I is 24 which takes the percentage of 20% in 120 specimens. With the number of 22 for group CH100, 19 for group CH150 and 13 for group CH200, the total number for mode II is 54 which accounts for 45% of 120 specimens. The numbers for mode III are 2, 3, 4 for group CH100, CH150 and CH200 respectively. And the total number for mode III is 9 which is 7.5% of 120 specimens.

Mode IV for the specimens under compression perpendicular to grain is different from the failure mode IV for the specimens under compression parallel to grain. As the shape for the crack line looks like

arc, mode IV could be called arc shape failure. Each specimen with this failure mode just has one arc shape crack line and the position for the line is random in one side. Group CH100 has 10 specimens damaged with mode IV. Group CH150 and CH200 have 5 and 14 specimens respectively. With the total number of 29, specimens of mode IV account for 24.17% of 120 specimens.

(a) Mode Ⅰ (b) Mode Ⅱ (c) Mode Ⅲ (d) Mode Ⅳ

**Figure 5:** Typical failure modes for axial compression strength failure

**Table 3:** Failure modes numbers for each group under compression perpendicular to grain

| Specimen group | Mode I | Mode II | Mode III | Mode IV | Total |
|---|---|---|---|---|---|
| CH100 | 6 | 22 | 2 | 10 | 40 |
| CH150 | 13 | 19 | 3 | 5 | 40 |
| CH200 | 5 | 13 | 4 | 14 | 36 |
| Total | 24 | 54 | 9 | 29 | 116 |

Seen from Tab. 3, 116 specimens belong to axial compression strength failure which account for 96.67% in 120 specimens. The other 4 specimens failed as the buckling failure and all these specimens belong to group CH200. Similar to the compression under compression parallel to grain, 50 by 50 by 200 mm is not good size for the specimen to measure the compression strength perpendicular to grain in a standard or code.

### *3.2 Calculation and Analysis of Test Results*

According to the mechanics of materials and GB/T 50329-2012 [36], the final calculation results for compression strength $f_c$, $E_c$, and Poisson's ratio $v$ for group specimens can be seen in Tab. 4. As the specimens under compression perpendicular to grain have two kinds of surfaces which have different mechanical properties, $v_{AC}$ and $v_{BD}$ are chosen for the Poisson's ratios of two series of the surfaces. $L$ is the length of the specimens and $s$ is the axial displacement of the specimens. The compression ratio can be calculated by $s/L$. COV means coefficient of variation; SDV means the standard deviation; CHV means characteristic value, calculated on the basis that 95% of samples exceed the characteristic value (mean ultimate value -1.645 x standard deviation). "CS" stands for all specimens under compression parallel to grain and "CH" stands for all specimens under compression perpendicular to grain.

**Table 4:** Test results for all specimens

| Group | | $f_c$/MPa | $E_c$/MPa | $v$ | $s/L$ | Group | | $f_c$/MPa | $E_c$/MPa | $v_{AC}$ | $v_{BD}$ | $s/L$ |
|---|---|---|---|---|---|---|---|---|---|---|---|---|
| CS100 | Mean | 102.1 | 14222 | 0.439 | 0.05 | CH100 | Mean | 54.40 | 4285 | 0.121 | 0.511 | 0.057 |
| | SDV | 7.97 | 1558 | 0.060 | 0.008 | | SDV | 8.56 | 679 | 0.021 | 0.105 | 0.013 |
| | COV | 0.078 | 0.110 | 0.137 | 0.152 | | COV | 0.157 | 0.159 | 0.177 | 0.206 | 0.226 |
| | CHV | 89.0 | 11659 | 0.340 | 0.038 | | CHV | 40.3 | 3167 | 0.086 | 0.337 | 0.036 |
| CS150 | Mean | 99.9 | 14015 | 0.404 | 0.042 | CH150 | Mean | 53.5 | 4270 | 0.110 | 0.505 | 0.051 |
| | SDV | 17.06 | 2114 | 0.038 | 0.008 | | SDV | 11.60 | 789 | 0.018 | 0.088 | 0.008 |
| | COV | 0.171 | 0.151 | 0.094 | 0.188 | | COV | 0.217 | 0.185 | 0.168 | 0.173 | 0.147 |
| | CHV | 71.8 | 10538 | 0.341 | 0.029 | | CHV | 34.4 | 2972 | 0.079 | 0.361 | 0.039 |
| CS200 | Mean | 96.3 | 13746 | 0.389 | 0.036 | CH200 | Mean | 49.1 | 4383 | 0.115 | 0.456 | 0.037 |
| | SDV | 15.85 | 1540 | 0.039 | 0.007 | | SDV | 8.32 | 853 | 0.020 | 0.107 | 0.008 |
| | COV | 0.165 | 0.112 | 0.101 | 0.201 | | COV | 0.169 | 0.195 | 0.178 | 0.236 | 0.221 |
| | CHV | 70.2 | 11212 | 0.325 | 0.024 | | CHV | 35.4 | 2979 | 0.081 | 0.279 | 0.024 |
| CS | Mean | 99.44 | 13994 | 0.411 | 0.049 | CH | Mean | 52.34 | 4313 | 0.115 | 0.491 | 0.043 |
| | SDV | 14.29 | 1754 | 0.051 | 0.013 | | SDV | 9.81 | 772 | 0.021 | 0.103 | 0.009 |
| | COV | 0.144 | 0.125 | 0.125 | 0.265 | | COV | 0.187 | 0.179 | 0.178 | 0.209 | 0.222 |
| | CHV | 75.9 | 11109 | 0.326 | 0.027 | | CHV | 36.2 | 3042 | 0.082 | 0.322 | 0.027 |

*3.2.1 Comparison of Compression Strength*

Fig. 6 plots the comparison of compression strength for two directions considering the length effect. Both the strength values for the compression parallel to grain and perpendicular to grain decrease with the increase of length values. The decrease speed between the length 100 mm and 150 mm is smaller than that between the length 150 mm and 200 mm. With the smallest COV values for both two compression directions, the discreteness for the shortest specimens is smallest among three groups. That is to say, length values have bigger influence on the longer specimens.

Combined all test results together, the mean strength values for compression parallel to grain and perpendicular to grain are 99.44 MPa and 52.34 MPa, with the standard deviation of 14.29 MPa, 9.81 MPa and coefficient of variation of 0.144, 0.187 respectively. The characteristic values for compression strength parallel to grain ( $f_{CS}$ ) and compression strength perpendicular to grain ( $f_{CH}$ ) are 75.9 MPa and 36.2 MPa respectively, and the relationship between them could be expressed as:

$$f_{CS}=2.1f_{CH} \tag{1}$$

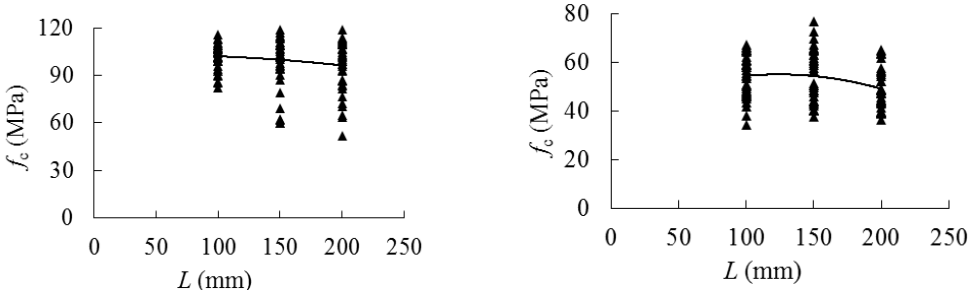


(a) Compression parallel to grain (b) Compression perpendicular to grain

**Figure 6:** Comparison of compression strength

*3.2.2 Comparison of Elastic Modulus*

Fig. 7 plots the comparison of elastic modulus for two directions considering the length effect. Both the trend lines in Fig. 6 and the COV values in Tab. 4 show that length values just have little effect on the elastic modulus no matter which compression direction it is. This effect can be omitted. That is to say that all these sizes are ok to measure the elastic modulus under compression. The size 50 mm × 50 mm × 100 mm is better from the point of saving materials.

Considering all test results together, the mean elastic modulus values for compression parallel to grain and perpendicular to grain are 13994 MPa and 4313 MPa, with the standard deviation of 1754 MPa, 772 MPa and coefficient of variation of 0.125, 0.179 respectively. The characteristic values of elastic modulus for compression parallel to grain ($E_{CS}$) and compression perpendicular to grain ($E_{CH}$) are 11109 MPa and 3042 MPa respectively, and the relationship between them could be expressed as:

$$E_{CS}=3.65E_{CH} \tag{2}$$

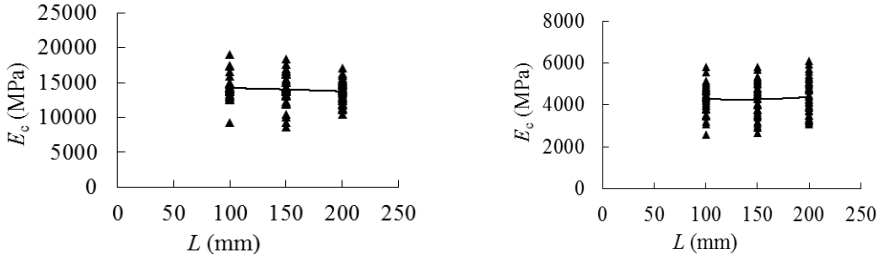


(a) Compression parallel to grain (b) Compression perpendicular to grain

**Figure 7:** Comparison of elastic modulus

*3.2.3 Comparison of Poisson's Ratio*

Fig. 8 plots the comparison of Poisson's ratio for two compression directions considering the length effect. Overall speaking, the values for Poisson's ratio decrease with the increase of the length no matter which compression direction it is. The values for $v$ and $v_{BD}$ are close to each other but these two kinds of values are pretty much bigger than the values for $v_{AC}$, and they are about four times of values for $v_{AC}$.

Combined all test results under compression parallel to grain together, the mean Poisson's ratio values is 0.411, with the standard deviation of 0.051 and coefficient of variation of 0.125. The characteristic values of Poisson's ratio for compression parallel to grain ($v$) is 0.326. As for the Poisson's ratio for PBSL under compression perpendicular to grain, the mean values for $v_{AC}$ and $v_{BD}$ are 0.115 and 0.491, with the standard deviation of 0.021, 0.103 and coefficient of variation of 0.178, 0.209 respectively. The characteristic values of $v_{AC}$ and $v_{BD}$ are 0.082 and 0.322 respectively. According to the characteristic values, the relationship between $v$, $v_{AC}$ and $v_{BD}$ could be expressed as:

$$v=v_{BD} \tag{3}$$

$$v_{BD}=3.93v_{AC} \tag{4}$$

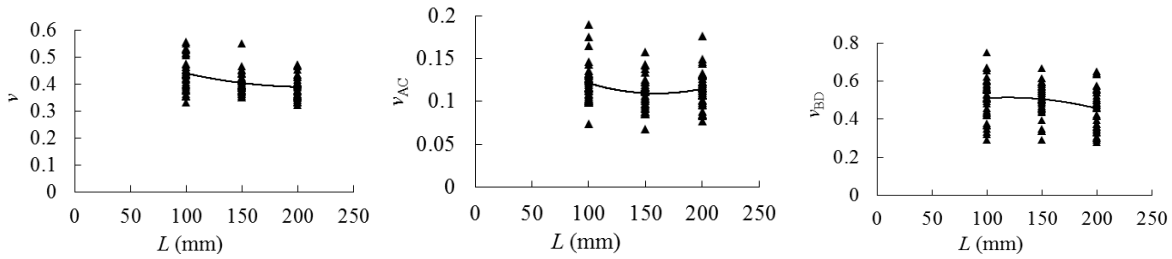


(a) Compression parallel to grain (b) Compression perpendicular to grain

**Figure 8:** Comparison of Poisson's ratio

*3.2.4 Comparison of Compression Ratio*

Fig. 9 plots how the length values influence on the compression ratio under two compression directions. As can be seen from the figures, the values for compression ratio decrease with the increase of the length no matter which direction it is. The slope of the trend lines for the compression ratio is bigger than that for all parameters discussed above. The CHV value for group CS100 is 0.038 which is very close to that value 0.036 for group CH100. It is also interesting to find that both the CHV values for group CS200 and CH200 are 0.024. Biggest compression ratio value means that the specimen with the length of 100 mm undertook fully compression which is close to the ideal axial compression. The size 50 mm × 50 mm × 100 mm should be good choice for the standard or code to measure the compression strength compared with other sizes.

Combined all test results together, the mean compression ratio values for compression parallel to grain and perpendicular to grain are 0.049 and 0.043, with the standard deviation of 0.013, 0.009 and coefficient of variation of 0.265, 0.222 respectively. However, it is interesting to find that the characteristic value of compression ratio for compression parallel to grain is equal to that for compression perpendicular to grain.

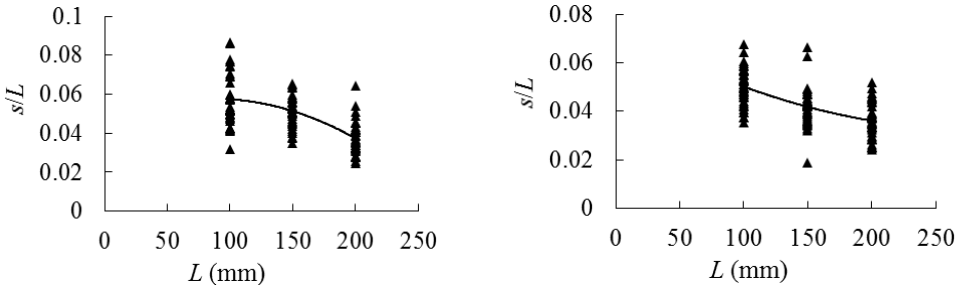


(a) Compression parallel to grain (b) Compression perpendicular to grain

**Figure 9:** Comparison of compression ratio

*3.2.5 Load-Displacement Curves*

Fig. 10 plots the load-displacement curves for all six groups. The failure process for the specimens under compression parallel to grain could be divided into four main stages which are elastic stage, elastic-plastic stage, plastic stage and decrease stage. However, there are only three stages for the failure process of the specimens under compression perpendicular to grain which are elastic stage, elastic-plastic stage and decrease stage. As for the specimens under compression perpendicular to grain, the load-displacement curves decreased once achieving the ultimate load. While for the specimens under compression parallel to grain, the ultimate load value will be kept for a certain time and it looks like plateau in the curves. PBSL materials have better ductility under compression parallel to grain than that under compression perpendicular to grain. The length value does not have too much influence on the

trend of the load-displacement curves. The load values decrease very quickly in the decrease stage for most of specimens no matter how long and which compression direction it is.

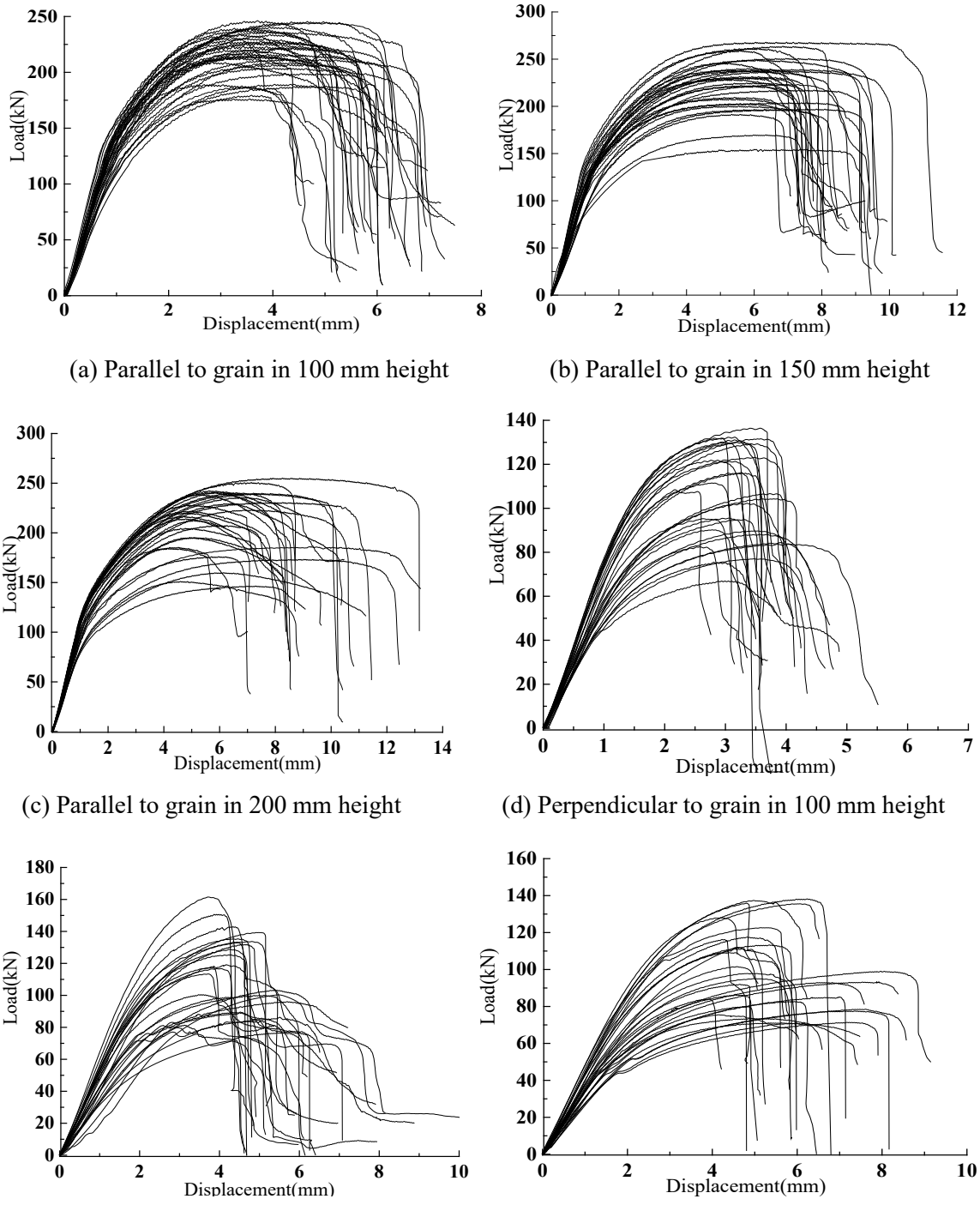


(a) Parallel to grain in 100 mm height (b) Parallel to grain in 150 mm height

(c) Parallel to grain in 200 mm height (d) Perpendicular to grain in 100 mm height

(e) Perpendicular to grain in 150 mm height (f) Perpendicular to grain in 200 mm height

**Figure 10:** Load displacement curves of specimens

*3.2.6 Stress-Strain Curves*

Fig. 11 plots the stress-strain curves for the test specimens from each group. The strain values were obtained from the strain gauges. As it is easy for the strain gauges to be broken or stop work when cracks

appeared, none decrease stages could be seen from Fig. 11. However, the overall trend for the curves in the first three stages give a good agreement with that for load displacement curves. It could be seen clearly that longer specimens have bigger discreteness for the curves.

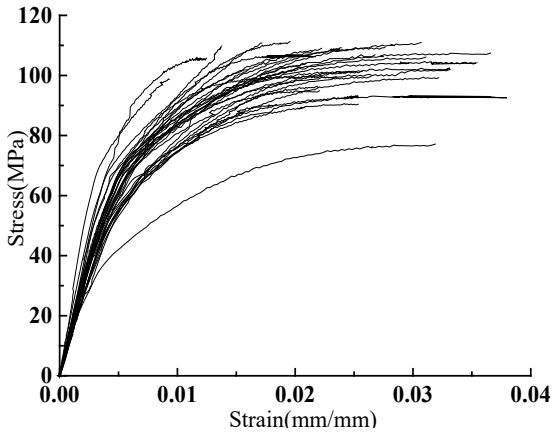


(a) Parallel to grain in 100 mm height

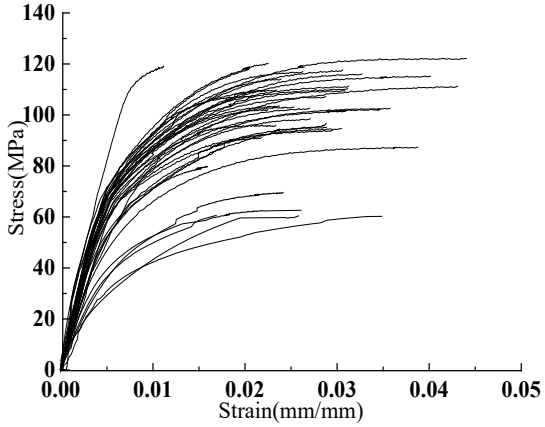


(b) Parallel to grain in 150 mm height

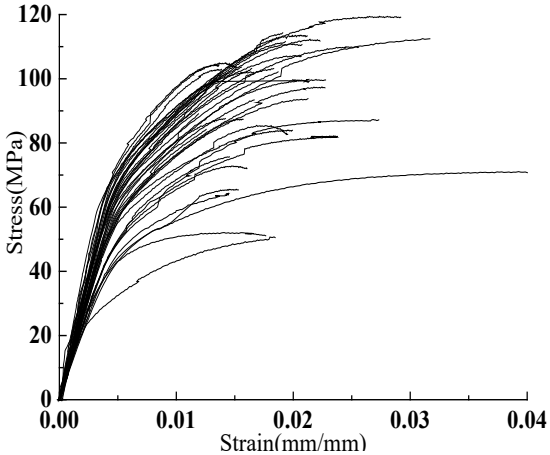


(c) Parallel to grain in 200 mm height

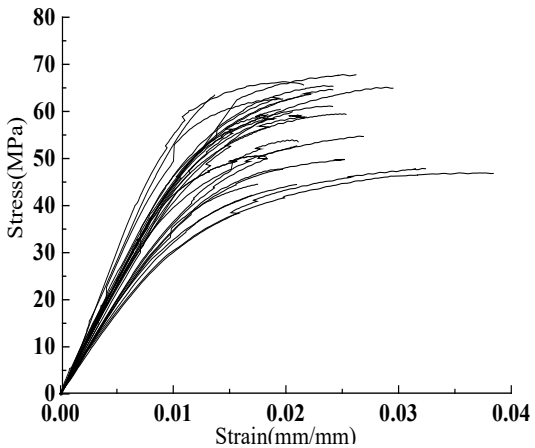


(d) Perpendicular to grain in 100 mm height

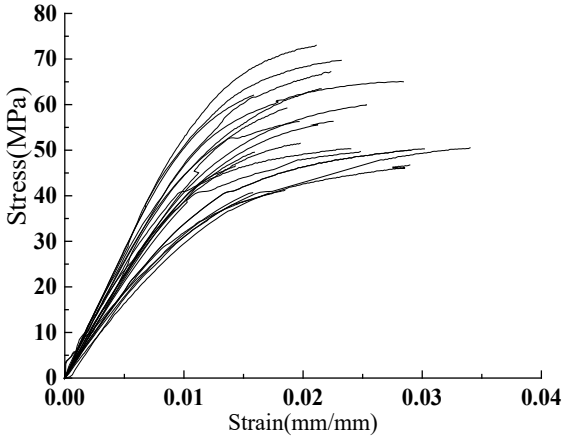


(e) Perpendicular to grain in 150 mm height

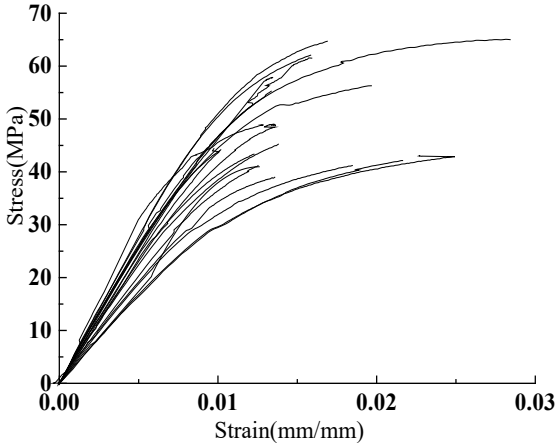


(f) Perpendicular to grain in 200 mm height

**Figure 11:** Stress-strain curves of specimens

## *4 Stress-Strain Relationship Model*

### *4.1 Stress-Strain Relationship Model Under Compressive Parallel to Grain*

As discussed above, the whole failure process could be divided into four stages for the specimens under compression parallel to grain. However, the period for the decrease stage is short and it does not have too much significance from the view of design point. When dealing with the test data for proposing the stress-strain relationship model, the compression failure process can be simplified into three stages which are elastic stage, elastic-plastic stage and plastic stage as shown in Fig. 12.

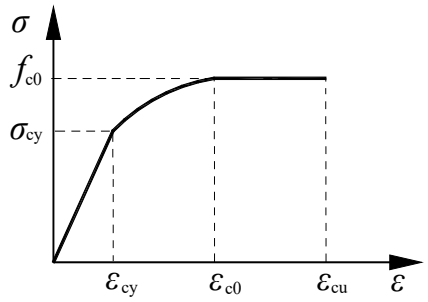


**Figure 12:** Stress-strain relationship model for PBSL under compression parallel to grain

By optimization, statistical regression and numerical analysis of all test results for PBSL under compression parallel to grain, the stress-strain relationship model could be expressed as following:

$$\sigma = \begin{cases} E_c \varepsilon & (0 \le \varepsilon \le \varepsilon_{cy}) \\ f_{c0}[1 + a(1 - \dfrac{\varepsilon}{\varepsilon_{c0}})^2] & (\varepsilon_{cy} \le \varepsilon \le \varepsilon_{c0}) \\ f_{c0} & (\varepsilon_{c0} \le \varepsilon \le \varepsilon_{cu}) \end{cases} \tag{5}$$

$$a = \frac{kn - 1}{(n-1)^2} \tag{6}$$

$$n = \frac{\varepsilon_{cy}}{\varepsilon_{c0}} \tag{7}$$

$$k = E_c \frac{\varepsilon_{c0}}{f_{c0}} = \frac{E_c}{\dfrac{f_{c0}}{\varepsilon_{c0}}} = \frac{E_c}{E_p} \tag{8}$$

where $\sigma$ is the stress value of the PBSL under compression parallel to grain; $E_c$ is the modulus of elasticity for PBSL; $E_p$ is the secant modulus for peak point $(\varepsilon_{c0}, f_{c0})$ ; $\varepsilon$ is the strain value of the PBSL; $\varepsilon_{cy}$ is the strain for the yield point; $\varepsilon_{c0}$ is the compression peak strain value; $f_{c0}$ is the compression peak stress value; $\varepsilon_{cu}$ is the ultimate maximum compression strain value.

The comparison between the proposed model and the test results for PBSL under compression parallel to grain can be seen from Fig. 13. As can be see clearly that the proposed model gives a good agreement with the rest results.

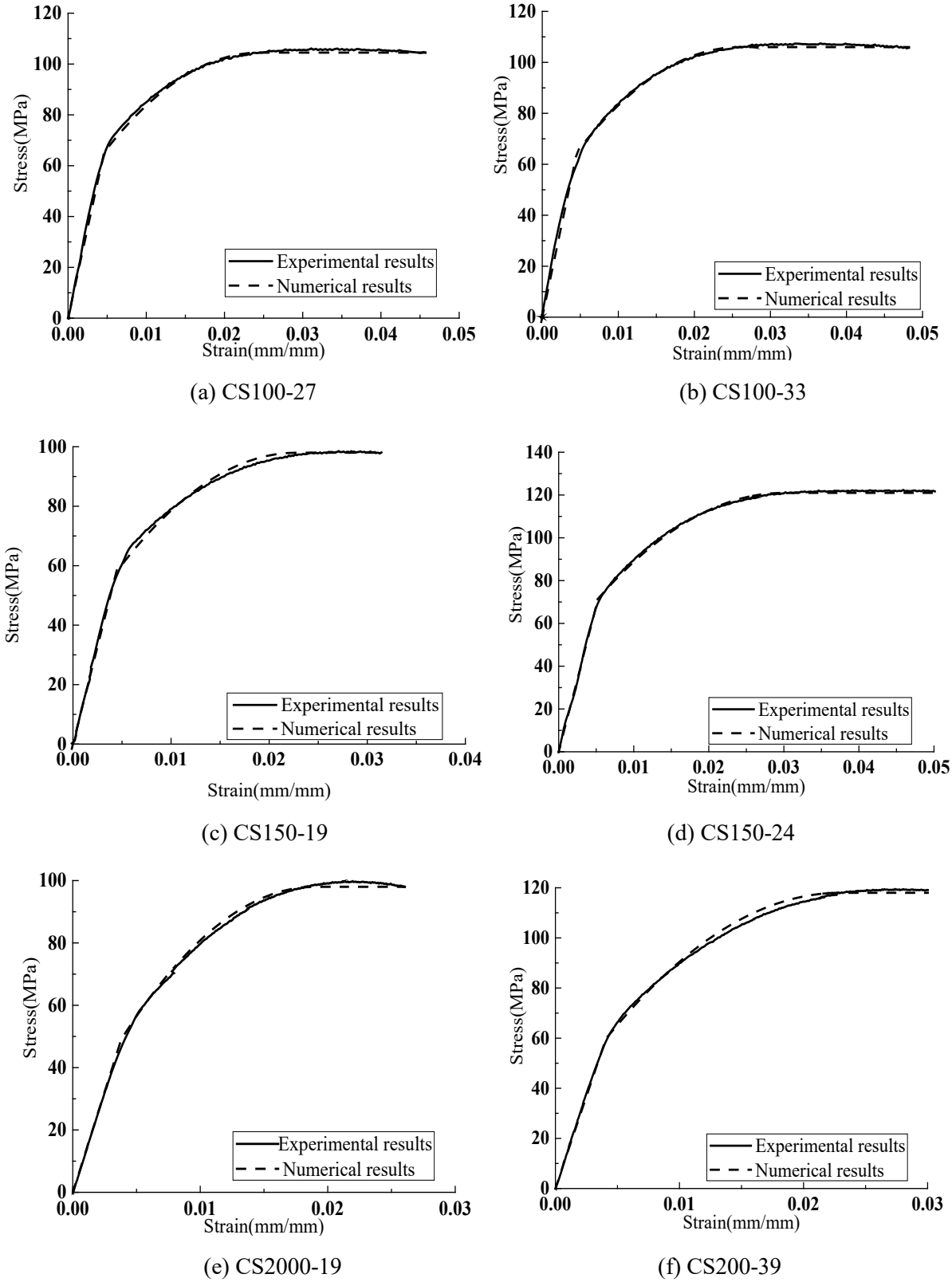


**Figure 13:** Comparison between the proposed model and the test results

### *4.2 Stress-Strain Relationship Model Under Compressive Perpendicular to Grain*

Similar reason to that for the specimens under compression parallel to grain, when dealing with the test data for proposing the stress-strain relationship model for PBSL under compression perpendicular to grain, the failure process can be simplified into two stages which are elastic stage, elastic-plastic stage as shown in Fig. 14.

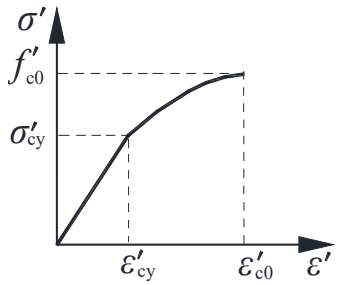


**Figure 14:** Stress-strain relation model for PBSL under compression perpendicular to grain

The stress-strain relationship model for PBSL under compression perpendicular to grain could be expressed as following:

$$\sigma' = \begin{cases} E'_c \varepsilon' & (0 \le \varepsilon' \le \varepsilon'_{cy}) \\ f'_{c0}[1 + a'(1 - \dfrac{\varepsilon'}{\varepsilon'_{c0}})^2] & (\varepsilon'_{cy} \le \varepsilon' \le \varepsilon'_{c0}) \end{cases} \tag{9}$$

$$a' = \frac{k'n' - 1}{(n' - 1)^2} \tag{10}$$

$$n' = \frac{\varepsilon'_{cy}}{\varepsilon'_{c0}} \tag{11}$$

$$k' = E'_c \frac{\varepsilon'_{c0}}{f'_{c0}} = \frac{E'_c}{\dfrac{f'_{c0}}{\varepsilon'_{c0}}} = \frac{E'_c}{E'_p} \tag{12}$$

where $\sigma'$ is the stress value of the PBSL under compression perpendicular to grain; $E'_c$ is the modulus of elasticity for PBSL; $E'$ is the secant modulus for peak point ($\varepsilon'_{c0}, \varepsilon'_{cy}$); $\varepsilon'$ is the strain value of the PBSL; $\varepsilon'_{cy}$ is the strain for the yield point; $\varepsilon'_{c0}$ is the compression peak strain value; $f'_{c0}$ is the compression peak stress value.

The comparison between the proposed model and the test results for PBSL under compression perpendicular to grain can be seen from Fig. 15. As can be seen clearly that the proposed model gives a good agreement with the rest results.

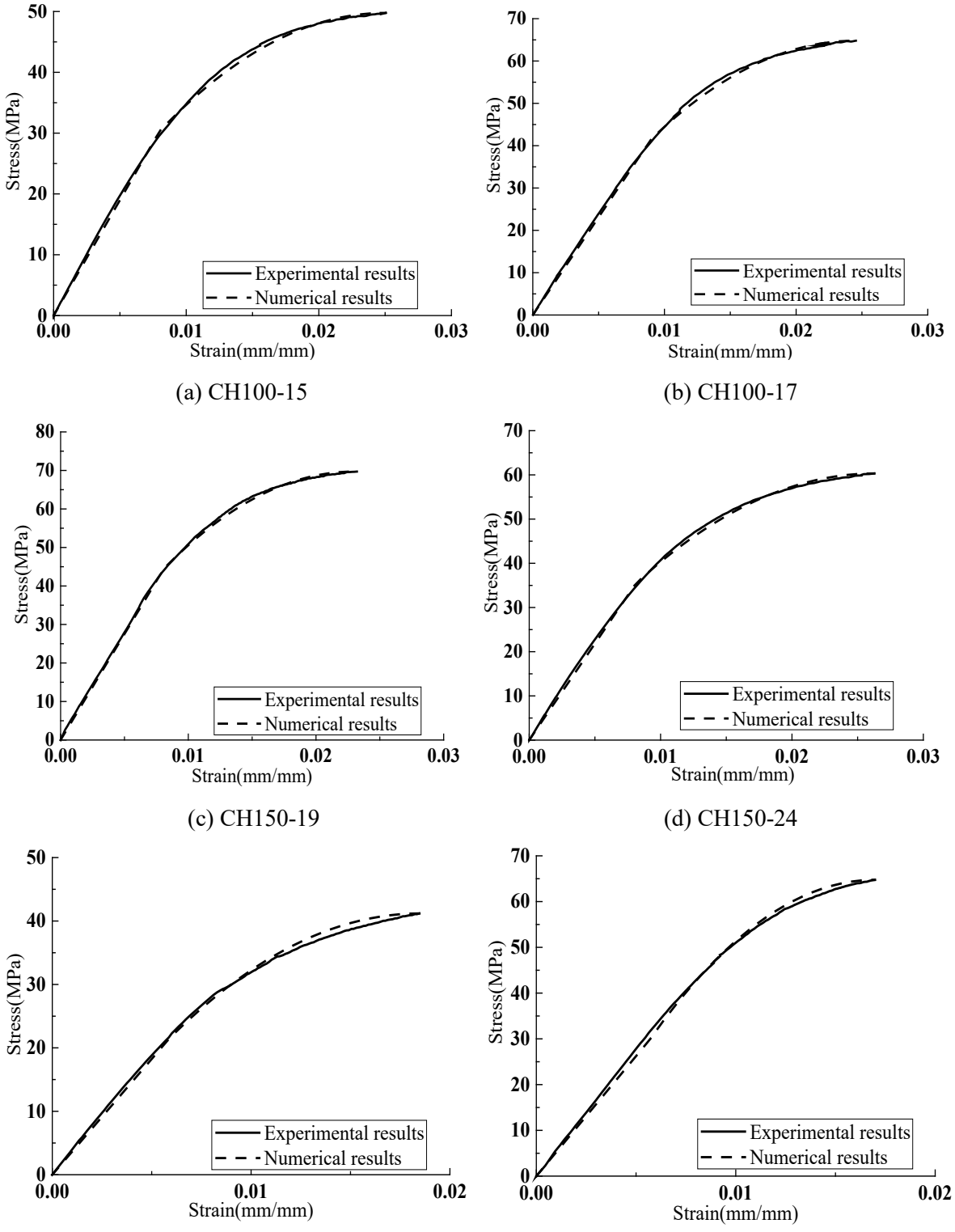


**Figure 15:** Comparison between the proposed model and the test results

## 5 Conclusions

In order to investigate the compression performance of parallel bamboo strand lumber manufactured from a new way, 240 axial compression tests have been carried out. Based on the analysis of the test data, the following conclusions can be drawn.

(1) Four typical failure modes could be classified both for the PBSL specimens under compression parallel to grain and perpendicular to grain. The former three modes are similar for the two compression directions. As the features for the fourth failure modes, all cracks developed along the vertical length direction of the specimen under compression parallel to grain while the final crack line shape for the specimen under compression perpendicular to grain looks like arc.

(2) As for the characteristic values, the compression strength parallel to grain is 2.1 times of the compression strength perpendicular to grain. The elastic modulus for compression parallel to grain is 3.64 times of the compression strength perpendicular to grain. While the compression ratios along two compression directions are equal to each other. The bigger Poisson ratios for one typical side surface is 3.93 times of that for another typical side surface for PBSL specimens under compression perpendicular to grain, and the bigger value is equal to that for PBSL specimens under compression parallel to grain.

(3) Length can influence the mechanical properties of the PBSL specimens. The size 50 mm × 50 mm × 100 mm should be good choice for the standard or code to measure the compression strength.

(4) PBSL materials have better ductility under compression parallel to grain than that under compression perpendicular to grain.

(5) Stress-strain relationship models were proposed for PBSL specimens under compression parallel to grain and perpendicular to grain, respectively. These proposed models gave a good agreement with the test results.

**Acknowledgments:** The research work presented in this paper is supported by the Natural Science Foundation of Jiang-su Province (No. BK20181402), the National Natural Science Foundation of China (51878354), National Key R&D Program of China, the Open Fund Project from Key Laboratory of Concrete and Pre-stressed Concrete Structure of Ministry of Education (Southeast university), the China Postdoctoral Science Foundation (2015M580382), Jiangsu Postdoctoral Science Foundation Project (1501037A), Qing Lan Project, and a Project Funded by the Priority Academic Program Development of Jiangsu Higher Education Institutions. Any research results expressed in this paper are those of the writer(s) and do not necessarily reflect the views of the foundations. The authors gratefully acknowledge, Feng Yang, Yixue Xie, Zhaoli Liu, Yunpeng Di, Jiang Zhu, Tao Song, Xiaoyan Zheng, Shaoyun Zhu, Liqing Liu, Dunben Sun, Jing Cao, Yanjun Liu and others from the Nanjing Forestry University for helping with the tests.

We declare that we do not have any commercial or associative interest that represents a conflict of interest in connection with the work submitted.

## References

1. Wang, Z., Wang, Y. L., Cao, Y., Gao, Z. Z. (2019). Measurements of the shear modulus of materials by the free-plate torsional mode shape method. *Journal of Testing and Evaluation, 47(2),* 1163-1181.
2. Wang, Z., Xie, W. B., Wang, Z. H., Cao, Y. (2018). Strain method for synchronous dynamic measurement of elastic, shear modulus and poisson's ratio of wood and wood composites. *Construction & Building Materials*, *182,* 608-617.
3. Li, H. T., Zhang, Q. S., Wu, G., Xiong, X. H., Li, Y. J. (2016). Review on laminated bamboo lumber. *Journal of Forestry Engineering, 1(6),* 110-116.
4. Huang, M. X., Zhang, X. C., Yu, W. J., Li, W. Z., Liu, X. M. et al. (2016). Mechanical properties and structure characterization of bamboo softened by high temperature steam. *Journal of Forestry Engineering, 1(4),* 64-68.

5. Chen, G., Zhou, T. Li, C. L., Zhang, Q. S., Li, H. T. (2016). Experimental study on the OSB webbed bamboo beams. *Journal of Nanjing Forestry University (Natural Science Edition), 40(5),* 121-125.
6. Li, Y. J., Xu B., Zhang, Q. S., Jiang, S. X. (2016). Present situation and the countermeasure analysis of bamboo timber processing industry in China. *Journal of Forestry Engineering, 1(1),* 2-7.
7. Li, H. T., Liu, R., Rodolfo, L., Wu, G., Wang, L. B. (2019). Eccentric compression properties of laminated bamboo lumber columns with different slenderness ratios. *Proceedings of the Institution of Civil Engineers-Structures and Buildings, 172(5),* 315-326.
8. Xiao, Y., Yang, R. Z., Shan, B. (2013). Production, environmental impact and mechanical properties of glubam. *Construction and Building Materials, 44(1),* 765-773.
9. Tian, L. M., Kou. Y. F., Hao, J. P. (2019). Flexural behavior of sprayed lightweight composite mortar-original bamboo composite beams: experimental study. *BioResources, 14(1),* 500-517.
10. Verma, C. S., Chariar, V. M. (2012). Development of layered laminate bamboo composite and their mechanical properties. *Composites Part B: Engineering, 43(3),* 1063-1069.
11. Correal J. F., Echeverry J. S., Ramírez F., Yamín L. E. (2014). Experimental evaluation of physical and mechanical properties of Glued Laminated Guadua angustifolia Kunth. *Construction and Building Materials, 73,* 105-112.
12. Chen, G., Li, H. T., Zhou, T., Li, C. L. (2015). Experimental evaluation on mechanical performance of OSB webbed parallel strand bamboo i-joist with holes in the web. *Construction and Building Materials, 101,* 91-98.
13. Su, J. W, Li, H. T., Yang, P., Zhang, Q. S., Chen, G. (2015). Mechanical performance study on laminated bamboo lumber column pier under axial compression. *China Forestry Science and Technology, 29(5),* 89-93.
14. Sharma, B., Gatóo, A., Bock, M., Ramage, M. (2015). Engineered bamboo for structural applications. *Construction and Building Materials, 81,* 66-73.
15. Zhou, J. W., Huang, D. S., Huang Z. R., Shen, Y. R. (2018). Experimental behavior of fabricated beam-column connection of bamboo frame under monotonic loading. *Journal of Forestry Engineering, 3(3),* 122-127.
16. Li, H. T., Qiu, Z. Y., Wu, G., Ottavia C., Wei, D. D. et al. (2019). Slenderness ratio effect on eccentric compression performance of parallel strand bamboo lumber columns. *Journal of Structural Engineering ASCE, 145(8),* 04019077.
17. Li, H. T., Su, J. W., Deeks, A. J., Zhang, Q. S., Wei, D. D. et al. (2015). Eccentric compression performance of parallel bamboo strand lumber column. *BioResources, 10(4),* 7065-7080.
18. Huang, H. Z. (2009). *The Study on Accelerated Aging Method and Aging Resistant Performance of Parallel Bamboo Strand Lumber (Ph.D. Thesis).* Nanjing Forestry University, Nanjing China.
19. Liang C. (2009). *Manufacturing Technology of Reconstituted Bamboo Lumber (Ph.D. Thesis).* Inner Mongolia Agricultural University, Huhehaote, China.
20. Naresworo, N., Naoto, A. (2000). Development of structural composite products made from bamboo I: fundamental properties of bamboo zephyr board. *Journal of Wood Science, 46,* 68-74.
21. Naresworo, N., Naoto, A. (2001). Development of structural composite products made from bamboo II: fundamental properties of laminated bamboo lumber. *Journal of Wood Science, 47(3),* 237-242.
22. Cui, H. X., Guan, M. J., Zhu, Y. X. (2012). The flexural characteristics of prestressed bamboo slivers reinforced parallel strand lumber (PSL). *Key Engineering Materials, 517,* 96-100.
23. Malanit, P., Barbu, M. C., Frühwald, A. (2011). Physical and mechanical properties of oriented strand lumber made from an Asian bamboo (Dendrocalamus asper Backer). *European Journal of Wood and Wood Products, 69(1),* 27-36
24. Zhou, A. P., Huang, Z. R., Shen, Y. R., Huang, D. S., Xu, J. U. (2018). Experimental investigation of mode-i fracture properties of parallel strand bamboo composite. *Bioresourses, 13(2),* 3905-3921.
25. Shangguan, W., Zhong, Y., Xing, X., Zhao, R., Ren, H. (2015). Strength models of bamboo scrimber for compressive properties. *Journal of Wood Science, 61,* 120-127.
26. Zhong, Y., Ren, H., Jiang, Z. (2016). Effects of temperature on the compressive strength parallel to the grain of bamboo scrimber. *Materials, 9(436),* 1-9.
27. Zhong Y., Jiang Z., Shangguan W., Ren H. (2014a). Design value of the compressive strength for bamboo fiber-reinforced composite based on a reliability analysis. *Bioresources, 9(4),* 7737-7748.

28. Ahmad, M., Kamke, F. A. (2011). Properties of parallel strand lumber from Calcutta bamboo (Dendrocalamus strictus). *Wood Science and Technology, 45(1),* 63-72.
29. Xu, M., Cui, Z., Chen, Z., Xiang, J. (2017). Experimental study on compressive and tensile properties of a bamboo scrimber at elevated temperatures. *Construction and Building Materials, 151,* 732-741.
30. Yu, Y., Huang, X., Yu, W. (2014). A novel process to improve yield and mechanical performance of bamboo fiber reinforced composite via mechanical treatments. *Composites Part B-Engineering, 56,* 48-53.
31. Yu, Y., Liu, R., Huang, Y., Meng, F., Yu W. (2017). Preparation, physical, mechanical, and interfacial morphological properties of engineered bamboo scrimber. *Construction and Building Materials, 157,* 1032-1039.
32. Wei, Y., Wu, G., Zhang, Q. S., Jiang, S, X. (2012). Theoretical analysis and experimental test of full-scale bamboo scrimber flexural components. *Journal of Civil, Architectural & Environmental Engineering, 34,* 140-145.
33. Wei, Y., Jiang, S. X., Lv, Q. F., Zhang, Q. Sh, Wang, L. B. et al. (2011). Flexural performance of glued laminated bamboo beams. *Advanced Materials Research, 168-170,* 1700-1703.
34. Zhong, Y., Wu, G., Ren, H., Jiang, Z. (2017). Bending properties evaluation of newly designed reinforced bamboo scrimber composite beams. *Construction and Building Materials, 143,* 61-70.
35. Chen, F., Deng, J., Li, X., Wang, G., Smith, L. M. et al. (2017). Effect of laminated structure design on the mechanical properties of bamboo-wood hybrid laminated veneer lumber. *European Journal of Wood Products, 75(3),* 439-448.
36. Standard for Test Methods of Timber Structures (GB/T 50329-2012) (2012). China Building Industry Press.